

# MICRO-RING RESONATORS AND THEIR APPLICATIONS

Sunami Morrison, Ameer I. Osman and Thusa Sivapatharajah

ECSE 430/540 Research Paper, Department of Electrical and Computer Engineering, McGill University,  
Montreal H3A 0G4, Canada

**ABSTRACT** - The simplicity of the structure of a micro-ring resonator combined with its ability to highly confine light into the waveguide makes it a practical choice for various applications. This paper gives a brief history and a concise theoretical discussion of silicon ring resonators of different types to understand the spectral transmission properties such as free spectral range (FSR), finesse, Q factors and coupling. Some of the applications that will be covered are firstly, spectral filters and switches that are used for data communication with the purpose of wavelength division multiplexing (WDM). Secondly, in biosensors, where they are used as perfect transducers to sense biochemicals. Finally, as active ring resonators in modulators. These applications will be explained in detail, while discussing about micro-ring resonators in this paper.

**INDEX TERMS** – Silicon photonics, microring resonators, integrated photonics, silicon on insulator.

## I. INTRODUCTION

Silicon photonics has recently made impressive progress in several devices and systems. This is attracting a lot of attention, where many applications are starting to require its use for fabricating compact and productive devices and systems. One of its important structure is the micro-ring resonator. Micro-ring resonators have the capability to confine power into the waveguide and is integrated in various applications. Silicon photonics is leading the way as a

fast and reliable method to handle such vast volume of data because of its bandwidth, scalability, reliability compactness and sensitivity. In this paper we investigate the applications of silicon microring resonators like filters and switches, modulators and biosensors. Furthermore, we analyze the data for filters and modulators.

## II. BACKGROUND AND THEORY

The first conception of a ring resonator was proposed by R. Ulrich & H.P Weber in 1972. The framework was set describing potential materials, preparation procedures and measurement methods.

A brief overview of a few key concepts before delving into ring resonators is required to understand this passive device and its limitations. These concepts include optical coupling, optical path length difference (OPD), free spectral range (FSR), finesse and quality factor (Q factor).

Optical coupling occurs when a linear waveguide is in proximity with the annular waveguide. Placing them in proximity allows the fields from the linear waveguide to emanate into the ring resonator and couple producing a field distribution within the ring resonator. Figure 1 depicts this phenomenon.

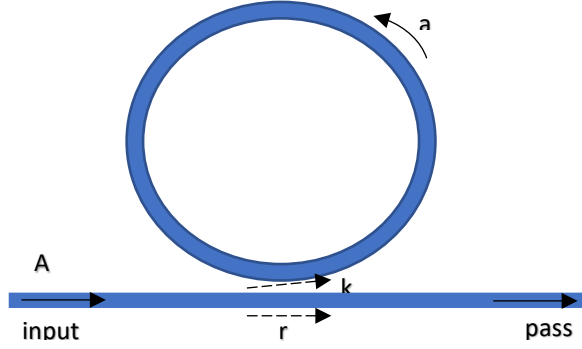


Fig. 1. Optical ring resonator & a linear waveguide, forming an all-pass ring resonator referenced from [1]

For this coupling to occur, the resonance condition dictated by the resonator geometry and the effective propagation wavelength must be met.

$$\text{OPD} = 2\pi R_{\text{neff}} = m\lambda_{\text{res}} \quad (2)$$

Where  $m$  is a non-zero integer and  $R$  is the radius of the ring. The OPD summarises the geometrical and material requirements of the resonator. The effective refractive index must be greater than the surrounding index in order to confine the coupled wave. Furthermore, there are a few cases of coupling depending on vectors  $r$ ,  $k$  and  $a$ , which are the self-coupling coefficient, the cross-coupling coefficient and single-pass amplitude transmission, respectively as depicted in Figure 1. The coupling cases will be discussed in the properties of a ring resonator section.

The Q factor is a measure of the dampening of the standing wave within the resonator. The standing wave is formed when the waves in the ring travel one round trip and interfere. The Q factor can be described mathematically as seen below:

$$Q = m\mathcal{F} = m\frac{V_{\text{FSR}}}{\delta} \quad (3)$$

Where  $\mathcal{F}$  is the finesse of the ring resonator,  $V_{\text{FSR}}$  is the free spectral range and  $\delta$  is the full-width half-maximum (FWHM) factor. The FSR is a measure of

the spectral separation of the wavelength modes that satisfy the resonance condition and hence can exist within the ring. The full-width half-maximum represents the mode's wavelength width at which the mode is at half of its peak intensity. The finesse is a ratio of the FSR and the FWHM and is hence dimensionless making the Q factor dimensionless as well. It represents a measure of the intensity of the modes relative to the mode's wavelength spread. As the Q factor is a measure of dampening, it provides an estimate of the round trips the waves propagate within the resonator before losing its energy to the resonator's internal losses.

### III. PROPERTIES OF RING RESONATORS

#### A. All-pass ring resonators

Figure 1 showcases an all-pass ring resonator. This configuration feeds the output of the ring resonator back into the linear waveguide, allowing all modes to propagate back in the linear waveguide. The characteristics of this all-pass filter (APF) can be derived from the ratio of output to input fields in the linear waveguide as seen below:

$$\frac{E_{\text{pass}}}{E_{\text{input}}} = e^{j(\pi+\phi)\frac{\alpha-re^{-j\phi}}{1-r\alpha e^{j\phi}}} \quad (4)$$

$$\Phi = \beta L \quad (5)$$

$$\alpha = \sqrt{e^{-\alpha L}} \quad (6)$$

Where  $\phi$  is the single-pass phase shift,  $L$  is the round-trip length,  $\beta$  is the propagation constant of the propagating mode and  $\alpha$  is the attenuation coefficient in  $\text{cm}^{-1}$ . The attenuation coefficient accounts for losses in ring propagation and coupling. Equation 4 provides us with an indication of the field's intensity after the APF. These equations only hold under the assumptions of matching fields, continuous wave operation and negligible back reflections. Squaring equation (4)

provides us with a measure of the field's intensity, as described by the intensity transmission  $T_n$  as seen below:

$$T_n = \frac{I_{pass}}{I_{input}} = \frac{a^2 - 2r\alpha\cos\phi + r^2}{1 - 2\alpha\cos\phi + r^2 a^2} \quad (7)$$

Vectors  $r^2$  and  $k^2$  indicate the passed and coupled power respectively. For the APF, it is assumed:

$$r^2 + k^2 = 1 \quad (8)$$

Indicating no losses in the phenomena of coupling. Over-coupling ( $T_n = 1$ ), Critical-coupling ( $T_n = 0$ ) and Under-coupling occur when  $r < a$ ,  $r = a$  and  $r > a$  respectively.

Generally, the APF shifts the phase of the wave as it is coupled temporarily to the ring then coupled back to the linear waveguide. This effective phase shift  $\phi$  can be calculated from the following equation:

$$\phi = \pi + \phi + \arctan\left(\frac{r\sin\phi}{\alpha - r\cos\phi}\right) + \arctan\left(\frac{r\alpha\sin\phi}{1 - r\alpha\cos\phi}\right) \quad (9)$$

The effective phase shift experienced for all coupling cases can be summarised graphically by plotting the effective phase delay against the single-pass phase shift as seen in Figure 2.

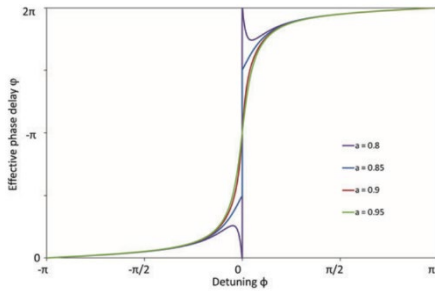


Fig. 2. Effective phase delay of the APF when  $r=0.85$  for different coupling cases [1]

The purple, blue, and red/green plots showcase respectively under-coupling, critical coupling and over-coupling. Figure 2 clearly displays the critical coupling causing a phase delay of  $\pi$  and over coupling

causing a continuous phase delay of  $2\pi$  as wave travels around the ring.

### B. Add-drop ring resonators

Add-drop ring resonators differ from APF resonators in that they have another linear waveguide dedicated to coupling certain wavelength modes, depending on the coupling between the drop linear waveguide and the ring and hence on their relative geometry and composition.

The fields in the pass and drop linear waveguides are described by their respective intensity transmission parameters under CW operation and matching fields assumptions:

$$T_{pass} = \frac{I_{pass}}{I_{input}} = \frac{r_2^2 \alpha^2 - 2r_1 r_2 \alpha \cos\phi + r_1^2}{1 - 2r_1 r_2 \alpha \cos\phi + (r_1 r_2 \alpha)^2} \quad (10)$$

$$T_{drop} = \frac{I_{drop}}{I_{input}} = \frac{(1 - r_1^2)(1 - r_2^2)\alpha}{1 - 2r_1 r_2 \alpha \cos\phi + (r_1 r_2 \alpha)^2} \quad (11)$$

### C. Spectral Characteristics

The spectral characteristics of both resonators are summarised in Figure 3.

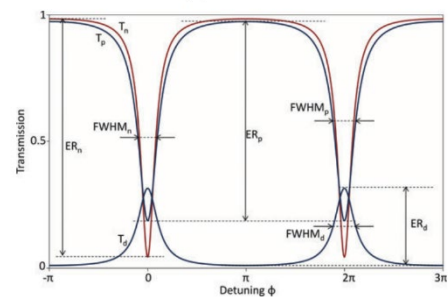


Fig. 3. Spectral characteristics of the all-pass resonator (left) and the add-drop resonator (right) as a function of transmission vs. single pass phase shift for  $a=0.85$  and  $r=r_1=r_2=0.9$  (under-coupled) [1]

The FWHM indicates the effective occupation of the spectrum of the given mode and can be derived

from their respective intensity transmission parameters:

$$\text{FWHM}_{\text{all-pass}} = \frac{(1-r_1r_2a)\lambda_{res}^2}{\pi n_g L \sqrt{ra}} \quad (12)$$

$$\text{FWHM}_{\text{add-drop}} = \frac{(1-r_1r_2a)\lambda_{res}^2}{\pi n_g L \sqrt{r_1r_2a}} \quad (13)$$

$$n_g = n_{\text{eff}} - \lambda_0 \frac{dn_{\text{eff}}}{d\lambda} \quad (14)$$

The FSR provides the spectral separation of the modes that exist in the ring resonator(s) and is given by:

$$\text{FSR} = \frac{\lambda_{res}^2}{n_g L} \quad (15)$$

The Finesse is a ratio of FSR to FWHM and thus provides a measure of the spread of the modes relative to the modal separation. The Q factor is a ratio of resonance wavelength to FWHM and thus provides a measure of the spread of the resonance relative to its respective modal wavelength.

In terms of energy, the finesse can be viewed as the number of round trips made by the wave before its total energy is depleted to 1/e of its initial value. Similarly, the Q factor is the number of periods of the wave at which its energy is depleted to 1/e of its initial value.

#### D. Losses and Coupling

There are two sources of losses, coupling losses and waveguide propagation losses. Coupling losses are mainly due to fabrication imperfections, including waveguide material and geometrical mismatch. The roundtrip loss  $A$  can be described with the following equation:

$$A^{\text{dB}} = A_{\text{propagation}}'L + 2A_{\text{coupling}} + 4A_{\text{bend}} \quad (16)$$

Where  $A_{\text{propagation}}'$  is the propagation loss in dB/cm, and  $A_{\text{bend}}$  is a loss specific to racetrack resonator, a

variation in which the ring elongates along the linear waveguide producing an oval shape. Equation 3 suggests that increasing  $L$  improves Q factor, but Equation 16 suggests that longer round-trip lengths  $L$  increase cumulative losses. Figure 4 showcases this optimization problem.

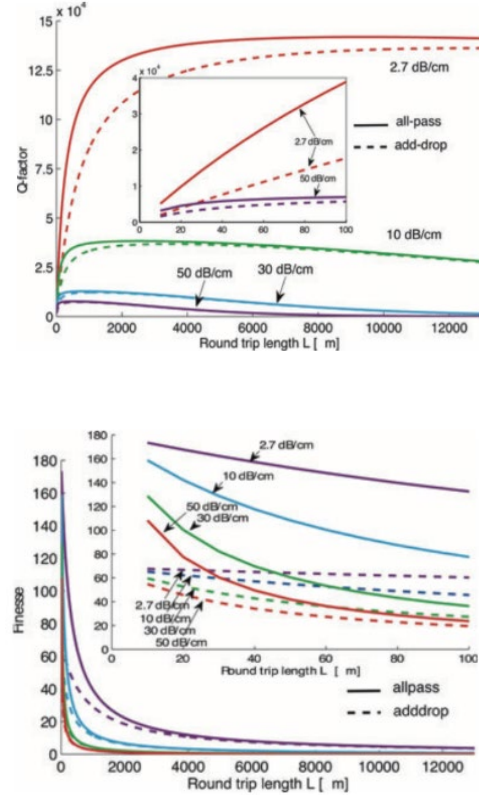


Fig. 4. (a) Propagation losses as a function of  $Q$ -factor to round trip length  $L$  (b) Propagation losses as a function of Finesse to round trip length  $L$ . For all-pass and add-drop configurations under critical coupling and air cladding ( $r_1=r_2=a$  for all-pass and  $r_1=r_2=a$  &  $r_2=0.99$  for add-drop) [1]

The lowest loss achievable is 2.7dB/cm at a Q factor of  $1.42 \times 10^5$  and a round trip length of 10mm. Furthermore, propagation losses may be minimized by high quality silicon-on-insulator material and processing.

#### IV. FIGURE OF MERITS - RING RESONATORS IN SILICON

##### A. Silicon Waveguides

Silicon waveguides deliver light through a silicon core surrounded by a silicon oxide bottom cladding and a low index top cladding (i.e. air or oxide). To fabricate effective silicon photonic devices, silicon-on-insulator (SOI) should have a high refractive-index contrast between the core and cladding. This makes the confinement stronger and allows the guided light to only bend slightly without radiating losses. In addition, the oxide layer should be thick enough to minimize leakage and allow the light to decay over the layer exponentially. As well as, the number of modes propagating through the waveguide depend on the dimensions of the waveguide [6]. Hence, if the width is too wide, multiple modes can propagate introducing loss. On the other hand, the refractive indices of the silicon and silicon dioxide are dispersive, i.e. depend on the wavelength, and the dimensions, i.e. height and width, of the waveguide contribute to confinement, so the effective index will also depend on the wavelength and dimensions of the waveguide [6]. Note that the effective index decreases as the wavelength increases, so less confinement of the optical mode because of its dispersive refractive index properties. As a result, propagating pulses are broadened and delayed. Furthermore, the fundamental TE mode is generally chosen to deliver light more efficiently. However, at the cost of the leakage of optical power, TM mode can be selected to allow less (back)scattering and achieve high-Q micro disk resonators [6].

##### B. Directional Couplers

Directional Couplers can couple light from a waveguide to a ring resonator by bringing two waveguides close. Let's consider a ring resonator consisting of a ring waveguide of radius ' $r$ ' between two rectangular waveguides for different coupling lengths ( $0\mu\text{m}$ ,  $1\mu\text{m}$  and  $1.5\mu\text{m}$ ). The ring waveguide is closed, so the wave propagating in it must fit constructive interference, such that the wave would couple in the ring. These wavelengths become the resonant wavelength in the output result of the ring resonator. The optical signal injected to the input port propagates through the rectangular waveguide to reach to the coupling region, which is at a minimum distance from the ring resonator. The coupled light at resonance wavelengths builds energy inside the ring. At other wavelengths, the electromagnetic wave passes through the coupling region and arrives at the output port.

For a ring of radius  $3\mu\text{m}$ , width of  $200\mu\text{m}$  and height of  $450\mu\text{m}$  and using a gap of  $0.02\mu\text{m}$  to prevent the ring from suffering any losses, the coupling length of the ring is varied from  $0\mu\text{m}$  to  $1.5\mu\text{m}$ . Figure 5 shows the confinement of the electric field in the waveguide and the relation between the coupling length against the wavelength. It can be concluded that as the coupling length of the ring resonator increases, more light is coupled into the ring due to increased exposure of passing wave to the ring structure to provide enough interaction length [8]. Therefore, the sensitivity of the resonator increases, and it can be evident that increasing coupling length results in sharper negative reflectance in spectrum.

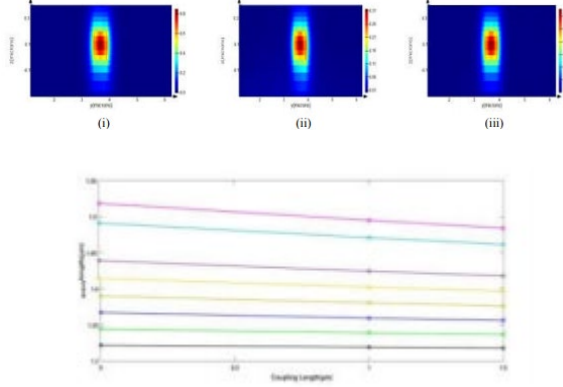


Fig. 5. (a) Electric field distribution as a function of position and wavelength for coupling lengths (i) LC=0μm (ii) LC=1μm (iii) LC=1.5μm (b) Coupling length as a function of wavelength [8]

#### D. Sensitivity

Sensitivity to dimensional variations when using a high index contrast technology for photonic devices is a major issue because of variations in the dimensions of the devices causing proportional shift in the spectral response. This is caused by non-uniformity while fabricating in lithography and etching [1]. In a ring resonator, the coupling gap is also a non-uniformity. Uniformity is met when the average width and height of the devices are matched over the circumference of the ring instead of the absolute local width and height. In other words, effective indices over the length of the cavity between two rings should be matched.

#### E. Tuning and Trimming

Tuning or trimming the device can help with the variation in the device's dimensions during fabrication. Resonance wavelength of a ring resonator can be tuned by thermal tuning. Thermal tuning is defined as a process in which the geometry of the system is altered by changing the operating frequency of the system using controlled thermal expansion. Hence the effective index can be modified to correct

the spectral response by supplying thermal energy to the device via micro-heaters placed on top or sides of the device [1]. This is done ensuring that enough isolation is provided to avoid optical loss. An efficient heater should be able to transfer heat to the device through isolating materials. Changing the effective index will cause a shift in the total wavelength response as desired [6]. After fabrication, resonance trimming can be done to change the spectral response. Resonance trimming requires changing the effective refractive index of the device by changing the refractive index of the core and clad materials [1]. A common method used is by locally injecting high optical power by a laser or by using photo-oxidation on the cladding layer.

### V. APPLICATIONS OF RING RESONATORS

#### A. Spectral Filters and Switches

Silicon microring resonators are used in optical networks as optical filters for telecommunication and data communication. An ideal ring resonator would be perfect for wavelength division multiplexing (WDM) system because its more compact. But it lacks the tolerance to changes to fabrication and temperature variations and hence it will require a good process control to make it reach its optimum working, i.e. for a ring to strike that specific wavelength without the use of large tuning rings. The shape of the resonance produced isn't good enough for a wavelength drop filter the uneven bandpass filter will cause signal distortion.

To overcome this issue, we use a higher order filter to give a uniform filter over a wider wavelength and maintaining a larger extinction ratio. In simple higher order wavelength filter would be to use two rings which are tuned individually to the same direction furthermore, when the two rings are detuned to the

opposite direction it behaves as a wavelength selective switch.

Higher order filters have several feedbacks which will improve the response of the filter. The filter having a good response can be characterized by a flatter top response and a faster roll off in passband. The response of a ring resonator as a filter can be improved by increasing the coupling constant. Higher order filters can either be serial or parallel cascade. In both cases the filter response is made better by special designs of the coupling constants of the cascade [9].

We investigate a compact second order filter that was simulated and designed for a flat top passband channel dropping [11]. The design takes into the propagation loss into account. After fabrication and characterizing it was observed for a ring resonator of radius  $2.5\mu\text{m}$  FSR of  $32\text{nm}$  at  $1.55\mu\text{m}$  and a bending radius of  $2.5\mu\text{m}$ .  $\kappa_p$  is the propagation power loss coefficient per round-trip in the microring resonator,  $\kappa^2$  is the power coupling coefficient between the bus waveguide and the resonator and  $\kappa_2^2$  mutual power coupling coefficients.  $\kappa_p^2 = 0.016$ ,  $\kappa^2 = 0.019$  and  $\kappa_2^2 = 0.025 \times (\kappa_p^2 + \kappa^2) = 0.0106$  and another similar design, but here  $\kappa_2^2 = 0.010$  this change is done to account for any fabrication defects.

It was seen that there is a resonance wavelength change of  $0.1\text{nm}$ . The design has achieved maximally flat pass band and a faster roll.

There is a low channel dropping loss of less than  $1\text{dB}$ , low add drop cross talk and high outside the band signal rejection of around  $30\text{-}40\text{dB}$ . During fabrication, there are bound to be imperfections which will lead to slightly shifted resonant frequency. This study takes the above-mentioned issue into account, and they have shown that a well-matched throughput response for a second order filter and be fabricated. Which can also be replicated for higher order filters.

In case of switching the two rings are designed such that in a straight waveguide the first ring selects the wavelength and the tuned second ring switches the wavelength to either a drop port or a non-used channel or an absorber.

### B. Label Free Biosensors

Biosensors use silicon on insulator (SOI) ring resonator for sensing analytes.

Typically, biological researchers depend on the detection of the analyte by easy to detect label (like a fluorescent dye) but for a label free system uses a transducer and that has the receptor molecule attached on the surface.

The sensing mechanism here depends on evanescent field. When the analytes meet cladding of the ring the analytes alter the effective refractive index which changes the resonant condition which further changes the resonant wavelength shift. The output light is connected to a photodetector or an optical spectrum analyzer [14].

For future work would be to integrate the ring resonator with laser source photodetector and electrical interconnects on the same chips and to improve packaging on the wafer level.

### C. Active Microring Modulators

A simple silicon electro-optic microring resonator (MMR) is a ring waveguide structure with a built-in p-n junction and is coupled to a silicon waveguide. If the cross of a silicon microring resonator is considered. The width is  $450\text{nm}$  and the height is  $200\text{nm}$  on a  $50\text{nm}$  width silicon slab.

The dimensions of the waveguide are much smaller than the wavelength i.e.  $1550\text{nm}$  the mode is highly confined to the waveguide. The ring diameter is  $12\mu\text{m}$  and the distance between the ring and the bus is  $200\text{nm}$  [10]. The refraction index changes in silicon when

voltage is applied i.e. it is an active device, and this changes the amplitude modulation carried out by the ring resonator. When compared to a Mach Zehnder interferometer (MZI) an MMR is much more compact. Furthermore, light in the ring resonator travels many times in the ring and it interacts with the carriers in the waveguide multiple times which is much lesser compared to an MZI. And because of this the power consumption also decreases. Also, in a ring resonator the light is modulated at a certain resonant wavelength or near resonant wavelength while allowing other wavelengths to pass by. An electro optic modulator is small, low footprint, low power consumption and are used for large scale integration in data centers.

$$\text{Normalised FOM} = \text{Normalised OMA} \times f(BW) \quad (17)$$

$$f(BW) = BW \quad (BW < DR \times 0.7)$$

$$f(BW) = DR \times 0.7 \quad (BW > DR \times 0.7). \quad (18)$$

$$\text{OMA} = (|S_t|^2)_{\max} - (|S_t|^2)_{\min} \quad [12] \quad (19)$$

$DR$ : Target data rate divided by Gbps

$BW$ : 3dB bandwidth divided by GHz,

$S_t$ : Transmitted field

$\tau_l$ : Decay time constant due to loss in ring resonator

$\tau_e$ : Decay time constant due to coupling with directional coupler

Normalised OMA: Optical modulation Amplitude normalized by the input optical power ( $P_{out}/P_{in}$ )

FOM: Figure of merit

0	22.42	24.65	2.637124	12
-1	22.88	24.62	2.637150	25
-2	23.12	24.65	2.637160	50

It was seen that the FOM of 25Gbps was much higher producing the biggest eye opening [13]. However, in the 50Gbps larger bandwidth was required and hence a clearer eye opening but smaller to that of the 25 Gbps. Therefore, 25 Gbps gives optimum results giving the best eye diagram.

Major difficulties faced with microring modulators is the sensitivity to temperature. There is more power consumption trying to maintain constant temperature for the microring resonator in data centers.

## VI. CONCLUSION

Microring resonators are compact, efficient and has multiple attractive properties mentioned in this paper which are popular for many applications. Ring resonators are very sensitive to environment, moreover, one of the issues faced with microring modulators is the sensitivity to temperature. Furthermore, there is more power consumption trying to maintain the optimum temperature for the microring resonator. Wafer level packaging is also a key issue that should be investigated the future, trying to integrate the laser, the chip and the photodetector all in one. With the advent of 5G, AI and internet of things the need for data centers to have high speed transceivers are necessary. Silicon photonics modulators, filters, switches and sensors are paving its way as a fast and reliable way to handle such vast volume of data and in the sensing field. Silicon photonics promises to keep up with the growing demand for higher bandwidth, scalability, sensitivity, reliability and low loss, which are essentials for data communications and sensing.

TABLE I

Normalized FOM for Different Bias Voltages [13]

Bias Voltage (V)	$\tau_l$ (ps rad <sup>-1</sup> )	$\tau_e$ (ps rad <sup>-1</sup> )	$N_{\text{eff}}$	Normalized FOM (Gbps)
------------------	----------------------------------	----------------------------------	------------------	-----------------------



## APPENDIX

Sunami: Sections 5 and 6

Ameer: Sections 2 and 3

Thusha: Sections 1 and 4

## REFERENCES

- [1] W. Bogaerts, "Silicon microring resonators," (in eng), *Laser and Photonics Reviews*, vol. 6, no. 1, p. 47, 2012.
- [2] P. Dong et al., "Low V pp, ultralow-energy, compact, high-speed silicon electro-optic modulator," *Optics express*, vol. 17, no. 25, pp. 22484-22490, 2009.
- [3] C. Roeloffzen, L. Zhuang, R. Heideman, A. Borreman, and W. Van Etten, "Ring resonator-based tunable optical delay line in LPCVD waveguide technology," in *Proc. 9th IEEE/LEOS Symp. Benelux*, 2005, pp. 79-82.
- [4] L. F. Stokes, "All-single-mode fiber resonator," (in eng), *Optics Letters*, vol. 7, no. 6, p. 288, 1982.
- [5] Y. Sun, "Optical ring resonators for biochemical and chemical sensing," (in eng), *Analytical and Bioanalytical Chemistry*, vol. 399, no. 1, p. 205, 2011.
- [6] Choi, Gwangho, "Modeling and Characterization of a Ring-Resonator based Silicon Photonic Sensor on Silicon-on-Insulator (SOI)", *Graduate Theses - Physics and Optical Engineering*, 2019.
- [7] R. Ulrich and H. P. Weber, "Solution-Deposited Thin Films as Passive and Active Light-Guides," *Appl. Opt.* 11, 428-434 (1972)
- [8] S. Sahai, A. D. Varshney, and S. K. Varshney, "Analysis, modeling and simulation of single all-silicon ring resonators and their comparison on the basis of their coupling lengths," *AIP Conference Proceedings*, vol. 2136, no. 1, p. 050011, 2019, doi: 10.1063/1.5120944.
- [9] Brent E. Little, Sai T. Chu, John V. Hryniewicz, and Philippe P. Absil, "Filter synthesis for periodically coupled microring resonators," *Opt. Lett.* 25, 344-346 (2000)
- [10] Xu, Q., Schmidt, B., Pradhan, S. *et al.* Micrometre-scale silicon electro-optic modulator. *Nature* 435, 325–327 (2005) doi:10.1038/nature03569
- [11] S. Xiao, M. H. Khan, H. Shen and M. Qi, "Silicon-on-Insulator Microring Add-Drop Filters With Free Spectral Ranges Over 30 nm," in *Journal of Lightwave Technology*, vol. 26, no. 2, pp. 228-236, Jan.15, 2008. doi: 10.1109/JLT.2007.911098
- [12] Hui Yu, Diqing Ying, Marianna Pantouvaki, Joris Van Campenhout, Philippe Absil, Yinlei Hao, Jianyi Yang, and Xiaoqing Jiang, "Trade-off between optical modulation amplitude and modulation bandwidth of silicon micro-ring modulators," *Opt. Express* 22, 15178-15189 (2014)
- [13] Kim, Y., et al. (2019). "Parametric optimization of depletion-type Si micro-ring modulator performances." *Japanese Journal of Applied Physics* 58(6): 062006.
- [14] Steglich, P.; Hülsemann, M.; Dietzel, B.; Mai, A. Optical Biosensors Based on Silicon-On-Insulator Ring Resonators: A Review. *Molecules* 2019, 24, 519.
- [15] Geuzebroek, D. H. and A. Driessen (2006). *Ring-Resonator-Based Wavelength Filters. Wavelength Filters in Fibre Optics.* H. Venghaus. Berlin, Heidelberg, Springer Berlin Heidelberg: 341-379.
- [16] Tobing, L. Y. M. and P. Dumon (2010). *Fundamental Principles of Operation and Notes on Fabrication of Photonic Microresonators. Photonic Microresonator Research and Applications.* I. Chremmos, O. Schwelb and N. Uzunoglu. Boston, MA, Springer US: 1-27.

